

A new chemical tool for exploring the physiological function of the PDE2 isozyme

Robert J. Chambers,^{a,*} Kristin Abrams,^a Norman Y. Garceau,^a Ajith V. Kamath,^a Christopher M. Manley,^c Susan C. Lilley,^a Douglas A. Otte,^a Dennis O. Scott,^b Alissa L. Sheils,^a David A. Tess,^b A. Samuel Vellekoop,^c Yan Zhang^a and Kelvin T. Lam^a

^aResearch Technology Center, Pfizer, Inc., 620 Memorial Drive, Cambridge, MA 02139, USA

^bGroton Laboratories, Pfizer, Inc., Eastern Point Road, Groton, CT 06340, USA

^cAlbany Molecular Research, Inc., 21 Corporate Circle, Albany, NY 12212, USA

Received 2 September 2005; revised 30 September 2005; accepted 3 October 2005

Available online 3 November 2005

Abstract—Oxindole (**2**) is a potent and selective PDE2 inhibitor with a favorable ADME, physiochemical and pharmacokinetic profile to allow for use as a chemical tool in elucidating the physiological role of PDE2.

© 2005 Elsevier Ltd. All rights reserved.

The phosphodiesterase (PDE) enzyme family controls intercellular levels of secondary messenger cAMP or cGMP through regulation of their hydrolysis. Phosphodiesterase Type II (PDE2) possesses a low affinity catalytic domain and an allosteric domain specific for cGMP. The low affinity catalytic site can hydrolyze both cAMP and cGMP with a lower apparent K_M for cGMP over cAMP. However, when cGMP binds to the allosteric site, the catalytic site undergoes a conformational change showing high affinity for cAMP. PDE2 is expressed throughout the body and therefore has a broad array of functions and potential therapeutic utility.¹ It has been shown that EHNA (erythro-9-(2-hydroxy-3-nonyl)adenine) (**1**) (Fig. 1), a potent adenosine deaminase inhibitor ($K_i = 10^{-9}$ M),² selectively inhibits PDE2.³ However, the use of EHNA (**1**) as a chemical tool in determining the pharmacological role of PDE2 is limited due to low PDE2 potency and high potency in inhibiting adenosine deaminase. A recent advancement in the development of PDE2 inhibitors is marked by the discovery that analogs of phosphatidylinositol 3-kinase (PI3K) inhibitor LY294002 inhibit PDE2 with potency approaching that of EHNA (**1**).⁴ Another recent advancement in the area is the report that Bay 60-7550, a potent and selective PDE2 inhibitor structur-

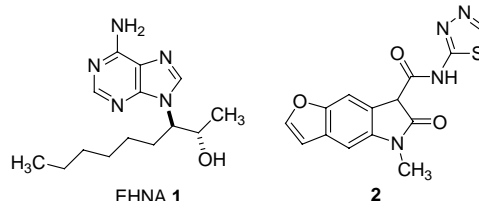


Figure 1. PDE2 inhibitors EHNA (**1**) and oxindole (**2**).

ally derived from EHNA (**1**), elevates intracellular cGMP in cultured neurons and is efficacious in animal models of memory and cognition.⁵ These recent findings prompt us to report that oxindole (**2**) is a potent and selective PDE2 inhibitor with a favorable pharmacological profile to allow the use as a chemical tool in further defining the role of PDE2 across a broad range of disease states.

In a comparative evaluation of potency and selectivity across the phosphodiesterase isozyme family, oxindole (**2**) was found to be a potent inhibitor of PDE2 being over an order of magnitude more potent than EHNA (**1**) and both compounds lacked significant inhibition of other isozymes indicating a high degree of selectivity toward PDE2 (Table 1).^{6,7} Also, **2** shows PDE2 potency higher than those reported for LY294002 analogs and PDE1 selectivity higher than that reported for Bay 60-7550.^{4,5}

Keywords: Phosphodiesterase; PDE2.

* Corresponding author. Tel.: +1 860 441 5695; fax: +1 860 441 1758;
e-mail: Robert.J.Chambers@pfizer.com

Table 1. Comparative PDE2 potency and selectivity of EHNA (**1**) and oxindole (**2**)

PDE isozyme	EHNA (1)	Oxindole (2)
PDE1 IC ₅₀ , nM (<i>n</i>)	>16,000 (1)	>16,000 (1)
PDE2 IC ₅₀ , nM (<i>n</i>) ^a	635 ± 134 (2)	40 ± 18 (9)
PDE3 IC ₅₀ , nM (<i>n</i>)	>16,000 (1)	>16,000 (1)
PDE4A IC ₅₀ , nM (<i>n</i>)	>16,000 (1)	>16,000 (1)
PDE4B IC ₅₀ , nM (<i>n</i>)	>16,000 (1)	>16,000 (1)
PDE4C IC ₅₀ , nM (<i>n</i>)	>16,000 (1)	>16,000 (1)
PDE4D IC ₅₀ , nM (<i>n</i>)	>16,000 (1)	>16,000 (1)
PDE5 IC ₅₀ , nM (<i>n</i>)	>16,000 (1)	>16,000 (1)
PDE8A IC ₅₀ , nM (<i>n</i>)	>16,000 (1)	>16,000 (1)
PDE8B IC ₅₀ , nM (<i>n</i>)	>16,000 (1)	>16,000 (1)
PDE9 IC ₅₀ , nM (<i>n</i>)	>16,000 (1)	>16,000 (1)
PDE10 IC ₅₀ , nM (<i>n</i>)	>16,000 (1)	>16,000 (1)
PDE11 IC ₅₀ , nM (<i>n</i>)	>16,000 (1)	11,600 (1)
PDE2 selectivity	>25X	290X

^aValues are means of a number (*n*) experiments with standard deviation.

In considering that **2** might interact with other pharmacological targets that in turn could then compromise interpretation of results from further in vitro and in vivo functional profiling, **2** was assayed for interaction against a collection of 54 receptors and ion channels where no significant level of binding relevant to its PDE2 potency was found (Table 2). In addition, oxindole (**2**) showed no inhibition of 5-lipoxygenase (5-LO) or cyclooxygenase (COX-1), two enzymes which other oxindole derivatives inhibit and derive anti-inflammatory activity (Table 3).^{8,9} The chemical structure of **2** displays proximal hydrogen bond donor and acceptor pairs which is associated with kinase inhibition which in turn would effect cell signaling.¹⁰ Against a panel of thirty kinases, **2** showed no significant inhibition relative to the level of PDE2 inhibition (Table 3).¹¹

In comparing the solubility and ADME properties of EHNA (**1**) and oxindole (**2**), both compounds showed an appreciable level of solubility and cell permeability however, oxindole (**2**) shows over a twofold increase in metabolic stability over EHNA (**1**) as measured by half-life in rat liver microsomes (Table 4).¹² In parental Madin–Darby canine kidney (MDCK) and transfectant multidrug resistant (MDR) overexpressing human p-glycoprotein (P-gp) cell lines, oxindole (**2**) showed a moderate rate of absorption with no apparent efflux.¹³

Having found a favorable solubility and ADME profile for oxindole (**2**), the in vivo pharmacokinetic profile was determined in rats, which showed a moderate rate of clearance and a low volume of distribution leading to a moderate half-life and level of oral bioavailability (Table 5).¹⁴ Furthermore, unbound plasma concentrations of oxindole (**2**) were achieved which exceeded its IC₅₀ value for over 2 h.

The synthesis of oxindole **2** proceeds via an eight-step linear sequence in a 33% overall yield starting from Metol **3**, an inexpensive and readily available starting material (Scheme 1). Acylation of **3** with chloroacetyl chloride occurs chemoselectively at the aniline nitrogen to give amide **4**.¹⁵ Cyclization of **4** by way of a intramo-

Table 2. Broad ligand binding profile of oxindole (**2**)

Target	% binding at 10 μM ^a
Adenosine A ₁	16
Adenosine A _{2a}	24
Adenosine A ₃	35
Adrenergic α ₁	0
Adrenergic α ₂	16
Adrenergic β ₁	15
Adrenergic β ₂	12
Norepinephrine Uptake	12
Angiotensin-I	11
Angiotensin-II	4
Benzodiazepine	11
Bradykinin B ₁	0
Bradykinin B ₂	5
Dopamine D ₁	5
Dopamine D ₂	12
Dopamine D ₃	0
Dopamine D ₄	0
Dopamine Uptake	11
GABA	3
GABA Uptake	8
AMPA	20
Kainate	0
NMDA	7
Histamine H ₁	7
Histamine H ₂	0
Histamine H ₃	0
MCR4	12
Muscarinic M ₁	9
Muscarinic M ₂	0
Muscarinic M ₃	0
Muscarinic M ₄	1
Choline Uptake	0
Neurokinin K ₁	0
Nicotinic (neuronal)	7
Nicotinic (muscle)	0
Opiate δ	3
Opiate κ	0
Opiate μ	3
PAF	21
Serotonin 5-HT _{1A}	23
Serotonin 5-HT _{2A}	15
Serotonin 5-HT _{2C}	0
Serotonin 5-HT ₃	0
Serotonin 5-HT ₄	0
Serotonin 5-HT ₇	0
Serotonin Uptake	0
Glucocorticoid	0
Thyroid hormone	0
Vasopressin V ₁	5
Vasopressin V ₂	13
Ca ²⁺ channel D (dihydro pyridine)	0
Ca ²⁺ channel D (diltiazem)	0
Ca ²⁺ channel L (verapamil)	0
Ca ²⁺ channel N	0

^aValues are from a single experiment with duplicate determinations.

lecular Friedel–Crafts alkylation occurs regioselectively to yield **5**.¹⁶ Acylation of **5** with chloroacetyl chloride followed by Fries rearrangement of ester **6** affords ketone **7**.¹⁷ Reduction of **7** and subsequent acid-catalyzed dehydration of alcohol **8** gives furan **9**. Acylation of **9** with diethylcarbonate followed by aminolysis of ester **10** with 2-aminothiadiazole affords **2** as a crystalline solid.

Table 3. Off target inhibition profile of oxindole (**2**)

Target	% inhibition at 10 μ M ^a
5-Lipoxygenase	35
Cyclooxygenase	0
MKK1	0
MAPK2	12
JNK1a1	0
SAPK2a	0
SAPK2b	5
SAPK3	7
SAPK4	13
RSK1	1
MAPKAP-K2	8
MSK1	6
PRAK	28
PKA	16
PKCa	13
PDK1	0
PKBa	14
SGK	0
p70S6K	23
GSK3 β	16
ROCK-II	20
AMPK	8
CHK1	0
CK2	32
PHK	0
LCK	5
CSK	5
CDK2	2
CK1	10
DYRK1A	53
NEK6	7
NEK2	0

^aValues are from a single experiment with duplicate determinations.

Table 4. Comparative ADME and solubility profile of EHNA (**1**) and oxindole (**2**)

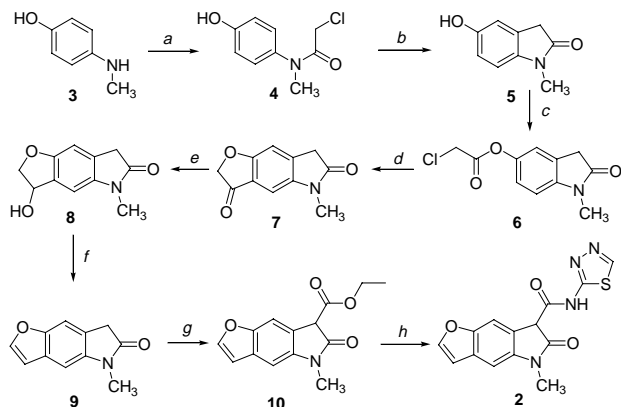
	EHNA (1)	Oxindole (2)
Rat liver microsome <i>t</i> _{1/2} (min)	31	83
Caco-2 apical <i>P</i> _{app} ($\times 10^{-6}$ cm/s)	34	5
Caco-2 basolateral <i>P</i> _{app} ($\times 10^{-6}$ cm/s)	18	32
MDCK apical <i>P</i> _{app} ($\times 10^{-6}$ cm/s)	NT	3.0
MDR basolateral <i>P</i> _{app} ($\times 10^{-6}$ cm/s)	NT	4.6
Turbidimetric solubility (pH 7, μ g/ml)	>65	55

NT, not tested.

Table 5. Rat pharmacokinetics of oxindole (**2**)

Clearance Cl (ml/min/kg)	8.8
Volume of distribution <i>V</i> _{dss} (L/kg)	0.1
Half life <i>t</i> _{1/2} (h)	1.6
<i>T</i> _{max} (h)	0.8
<i>C</i> _{max} (ng/ml)	8303
Oral bioavailability % F	41

Oxindole (**2**) is a potent and selective PDE2 inhibitor that possesses a suitable solubility and in vitro ADME profile leading to a moderate level of in vivo oral bioavailability and half-life in rats. Against a panel of 54 receptors and ion channels, oxindole (**2**) shows no significant interaction nor is effective in inhibiting 5-li-



Scheme 1. Reagents and conditions: (a) ClCOCH_2Cl , TEA, DMAP, DMF, 0 °C, 83%; (b) AlCl_3 , 180 °C, 89%; (c) ClCOCH_2Cl , Py CH_2Cl_2 , 0 °C, 94%; (d) AlCl_3 , 180 °C, 76%; (e) NaBH_4 , MeOH, 0 °C, 92%; (f) TFA, MeCN, 20 °C, 88%; (g) $(\text{EtO})_2\text{CO}$, Na, EtOH, reflux, 97%; (h) 2-amino-1,3,4-thiadiazole, 4 Å Sieves, PhH, reflux, 80%.

poxygenase (5-LO) or cyclooxygenase (COX-1), two enzymes which other oxindole derivatives inhibit and derive anti-inflammatory activity. In regard to mediating off target cell signalling pathways, oxindole (**2**) showed no significant inhibition against a panel of 30 kinases. Thus, oxindole (**2**) is positioned to be a useful chemical tool in defining the role of PDE2 in a broad range of disease states.

References and notes

- Juijls, D. M.; Soderling, S.; Burn, F.; Beavo, J. A. *Rev. Physiol. Biochem. Pharmacol.* **1999**, *135*, 67.
- Baker, D. C.; Hanvey, J. C.; Hawkins, L. D.; Murphy, J. *Biochem. Pharm.* **1981**, *30*, 1159.
- Podzuweit, T.; Nennstiel, P.; Mueller, A. *Cell. Signal.* **1995**, *7*, 733.
- Abbott, B. M.; Thompson, P. E. *Bioorg. Med. Chem. Lett.* **2004**, *14*, 2847.
- Boess, F. G.; Hendrix, M.; van der Staay, F.-J.; Erb, C.; Schreiber, R.; van Staveren, W.; de Vente, J.; Prickaerts, J.; Blokland, A.; Koenig, G. *Neuropharmacology* **2004**, *47*, 1081.
- For preparations of PDE1, PDE2, PDE3, PDE4A, PDE4B, PDE4C, PDE4D, PDE5, PDE8A, PDE8B, PDE9, PDE10, and PDE11 isozymes, see (a) Mueller, H. W.; Clapshaw, P. A.; Seifert, W. *FEBS Lett.* **1981**, *131*, 37; (b) Dickinson, N.; Jang, E.; Haslam, R. *Biochem. J.* **1997**, *323*, 371; (c) Cohan, V.; Showell, H.; Fisher, D.; Pazoles, C.; Watson, J.; Turner, C.; Cheng, J. *J. Pharm. Exp. Ther.* **1996**, *278*, 1356; (d) Fisher, D.; Smith, J.; Pillar, J.; Denis, S.; Cheng, J. *Biochem. Biophys. Res. Commun.* **1998**, *246*, 570; (e) Hayashi, M.; Matsushima, K.; Ohashi, H.; Tsunoda, H.; Murase, S.; Kawarada, Y.; Tanaka, T. *Biochem. Biophys. Res. Commun.* **1998**, *250*, 751; (f) Fisher, D.; Smith, J.; Pillar, J.; Denis, S.; Cheng, J. *J. Biol. Chem.* **1998**, *273*, 15559; (g) Fujishige, K.; Kotera, J.; Omori, K. *Eur. J. Biochem.* **1999**, *266*, 1118; (h) Fawcett, L.; Baxendale, R.; Stacey, P.; McGrouther, C.; Harrow, I.; Soderling, S.; Hetman, J.; Beavo, J. *Proc. Natl. Acad. Sci. U.S.A.* **2000**, *97*, 3702.
- EHNA (**1**) and oxindole (**2**) were evaluated for phosphodiesterase inhibition activity using a scintillation proximity assay (SPA) in 96-well plates. The PDE SPA

- yttrium silicate beads (Amersham Biosciences[®]) bind preferentially to the linear nucleotide compared to the cyclic nucleotide. In the case of PDE2, ³H-cGMP and unlabeled cGMP are added to the reaction and when the product, ³H-GMP, is in close proximity to the beads, the scintillant within the bead is excited, which is detected using a Packard scintillation counter. The enzyme concentration used is in the linear range and the K_M of the enzyme was determined (15 μM). The final substrate concentration is <1/3 of K_M (1 μM) so that IC₅₀ values would approximate the K_i values (a) Bardelle, C.; Smales, C.; Ito, M.; Nomoto, K.; Wong, E. Y. M.; Kato, H.; Saeki, T.; Staddon, J. M. *Anal. Biochem.* **1999**, *275*, 148; (b) Laliberte, F.; Han, Y.; Govindarajan, A.; Giroux, A.; Liu, S.; Bobechko, B.; Lario, P.; Bartlett, A.; Gorseth, E.; Gresser, M.; Huang, Z. *Biochemistry* **1997**, *36*, 2968; (c) Card, G. L.; England, B. P.; Suzuki, Y.; Fong, D.; Powell, B.; Lee, B.; Luu, C.; Tabrizad, M.; Gillette, S.; Ibrahim, P. N.; Artis, D. R.; Bollag, G.; Milburn, M.; Kim, S.-H.; Schlessinger, J.; Zhang, K. Y. *J. Structure* **2004**, *12*, 2233.
8. Oxindole (**2**) was evaluated in a broad ligand panel by Cerep (France) and also for 5-lipoxygenase (5-LO) and cyclooxygenase (COX-1) inhibition activities.
 9. (a) Mylari, B. L.; Carty, T. J.; Moore, P. F.; Zembrowski, W. *J. J. Med. Chem.* **1990**, *33*, 2019; (b) Wiseman, E. H.; Chiaini, J.; McManus, J. M. *J. Med. Chem.* **1973**, *16*, 131.
 10. (a) Giovanna, S. *Drug Discov. Today* **2002**, *7*, 601; (b) Dumas, J. *Exp. Opin. Ther. Patents* **2001**, *11*, 405; (c) Garcia-Echeverria, C.; Traxler, P.; Evans, D. B. *Med. Res. Rev.* **2000**, *20*, 28; (d) Traxler, P.; Furet, P. *Pharmacol. Ther.* **1999**, *82*, 195.
 11. Oxindole (**2**) was evaluated in a panel of kinases by P. Cohen, University of Dundee, Dundee, Scotland, UK
 - Davies, S. P.; Reddy, H.; Caivano, M.; Cohen, P. *Biochem. J.* **2000**, *351*, 95.
 12. For rat liver microsome assay see: (a) Obach, R. S.; Baxter, J. G.; Liston, T. E.; Silber, B. M.; Jones, B. C.; MacIntyre, F.; Rance, D. J.; Wastall, P. *J. Pharm. Exp. Ther.* **1997**, *283*, 46; (b) Conradi, R. A.; Wilkinson, K. F.; Rush, B. D.; Hilgers, A. R.; Ruwart, M. J.; Burton, P. S. *Pharm. Res.* **1993**, *10*, 1790; For CACO-2 cell permeability assay see: (c) Lipinski, C. A. *Meth. Prin. Med. Chem.* **2003**, *18*, 215; For turbidimetric solubility determination see: (d) Brooker, P. J.; Ellison, M. *Chem. Ind.* **1974**, *19*, 285.
 13. (a) Guo, A.; Marinaro, W.; Hu, P.; Sinko, P. *J. Drug Metab. Disp.* **2002**, *30*, 457; (b) Luo, F. R.; Paranjpe, P. V.; Guo, A.; Rubin, E.; Sinko, P. *Drug Metab. Disp.* **2002**, *30*, 763; (c) Karykari, C. S.; Eddington, N. D.; Garimella, T. S.; Tushar, S.; Gubbins, P. P.; Dowling, T. C. *Pharmaco-therapy* **2003**, *23*, 436; (d) Williams, G. C.; Knipp, G. T.; Sinko, P. *J. J. Pharm. Sci.* **2003**, *92*, 1957; (e) Wang, Q.; Rager, J. D.; Weinstein, K.; Kardos, P. S.; Dobson, G. L.; Li, J.; Hidalgo, I. *J. Int. J. Pharm.* **2005**, *288*, 349.
 14. Sprague-Dawley rats were dosed with oxindole (**2**) intravenously, 1 mg/kg in EtOH:PEG 400:H₂O (1:4:5) and orally, 30 mg/kg in 0.5% methylcellulose and plasma samples were drawn at 0.083, 0.25, 0.5, 1, 2, 4, 6, and 8 h post dose for analysis. Two animals were used for each dosing route and mean plasma concentrations were used in subsequent calculations.
 15. Clark, N. G.; Hams, A. F. *Biochem. J.* **1953**, *55*, 839.
 16. (a) Julian, P. L.; Pikl, J. *J. Am. Chem. Soc.* **1935**, *57*, 563; (b) Julian, P. L.; Pikl, J.; Wantz, F. E. *J. Am. Chem. Soc.* **1935**, *57*, 2026.
 17. (a) Wright, S. W.; McClure, L. D.; Hageman, D. L. *Tetrahedron Lett.* **1996**, *37*, 4631(b) Chambers, R. J.; Lam, K. T. WO 2005041957, 2005; *Chem. Abstr.* **2005**, *142*, 463708.;